Calcium-Dependent Catalytic Activity of a Novel Phytase from *Bacillus amyloliquefaciens* DS11

Byung-Chul Oh,[‡,§] Byeong S. Chang,[||] Kwan-Hwa Park,[§] Nam-Chul Ha,[⊥] Hyung-Kwoun Kim,[‡] Byung-Ha Oh,[⊥] and Tae-Kwang Oh*[,‡]

Microbial Genomic Laboratory, Korea Research Institute of Bioscience and Biotechnology, P.O. Box 115, Yusong, Taejon 305-600, South Korea, Research Center for New Bio-Materials in Agriculture and Department of Food Science and Technology, Seoul National University, Suwon 441-744, South Korea, National Creative Research Initiative Center for Biomolecular Recognition, Department of Life Science, and Division of Molecular and Life Science, Pohang University of Science and Technology, Pohang, Kyungbuk, 790-784, South Korea, and Department of Pharmaceutics and Drug Delivery, Amgen, Inc., Thousand Oaks, California 91320

Received March 23, 2001; Revised Manuscript Received June 1, 2001

ABSTRACT: The thermostable phytase from *Bacillus amyloliquefaciens* DS11 hydrolyzes phytate (*myo*-inositol hexakisphosphate, IP6) to less phosphorylated *myo*-inositol phosphates in the presence of Ca^{2+}. In this report, we discuss the unique Ca^{2+}-dependent catalytic properties of the phytase and its specific substrate requirement. Initial rate kinetic studies of the phytase indicate that the enzyme activity follows a rapid equilibrium ordered mechanism in which binding of Ca^{2+} to the active site is necessary for the essential activation of the enzyme. Ca^{2+} turned out to be also required for the substrate because the phytase is only able to hydrolyze the calcium−phytate complex. In fact, both an excess amount of free Ca^{2+} and an excess of free phytate, which is not complexed with each other, can act as competitive inhibitors. The Ca^{2+}-dependent catalytic activity of the enzyme was further confirmed, and the critical amino acid residues for the binding of Ca^{2+} and substrate were identified by site-specific mutagenesis studies. Isothermal titration calorimetry (ITC) was used to understand if the decreased enzymatic activity was related to poor Ca^{2+} binding. The pH dependence of the V_{max} and V_{max}/K_m consistently supported these observations by demonstrating that the enzyme activity is dependent on the ionization of amino acid residues that are important for the binding of Ca^{2+} and the substrate. The Ca^{2+}-dependent activation of enzyme and substrate was found to be different from other histidine acid phytases that hydrolyze metal-free phytate.

Phytate[1] (*myo*-inositol 1,2,3,4,5,6-hexakisphosphate, IP6) is the principal storage form of phosphorus in plants, particularly in cereal grains and legumes (*1*). It typically represents approximately 75%−80% of the total phosphorus found in nature. Phytate is a strong chelator of cations and binds minerals such as Ca^{2+} (*2*), Zn^{2+} (*3*, *4*), and Fe^{2+} (*5*), making them unavailable for absorption in the intestine of the monogestric animal, e.g., human, pig, poultry, and fish. The intake of large amounts of foods rich in phytate may cause several mineral deficiency symptoms (*6*). The bioavailability of minerals and phosphorus in the cereals will improve if phytate is degraded (*7*, *8*), and the removal of phytate from plant foods thus becomes of nutritional significance. It is also becoming evident that the inositol phosphate intermediates have beneficial biological activities. Recently, it was shown that the breakdown products of phytate containing the inositol 1,2,3-trisphosphate also have antioxidant functions (*9*, *10*). Inositol 1,2,3,6-tetrakisphosphate also has second messenger activity in mobilizing calcium (*11*, *12*) and increases the absorption of calcium from the diet in rats (*13*).

The primary enzymes responsible for the degradation of phytate are phytases. Phytase has been studied intensively in the past few years because of the great interest in using such enzymes for reducing the phytate content in animal feed and food for human consumption. The phytases are a subfamily of high molecular weight histidine acid phosphatases that can hydrolyze phytate to less phosphorylated *myo*-inositol phosphates and free orthophosphate (*14*). Several fungal, bacterial, and plant phytases belong to the histidine acid phosphatase (HAP) class of enzymes (*14*, *15*). All of these phytases share a conserved active site motif, RHGXRXP, unique to this class of enzymes (*16*). These HAPs are also classified as 3-phytase (EC 3.1.3.8) and 6-phytase (3.1.3.26) on the basis of their specificity of removal of the first phosphate group of phytate. A detailed reaction mechanism of the *Escherichia coli* phytase has been elucidated by mutagenesis (*17*, *18*) and crystallographic studies using both transition state analogue complexes and enzyme−substrate complexes (*17*−*19*). The region of the active site contains mostly positively charged groups, which indicates favorable binding of phytate, but unfavorable binding of metal−phytate complexes due to electrostatic

* To whom correspondence should be addressed. Phone: 82-42-860-4374. Fax: 82-42-860-4595. E-mail: otk@mail.kribb.re.kr.
‡ Korea Research Institute of Bioscience and Biotechnology.
§ Seoul National University.
|| Amgen, Inc.
⊥ Pohang University of Science and Technology.

[1] Abbreviations: phytate or metal-free phytate, *myo*-inositol 1,2,3,4,5,6-hexakisphosphate; Ca−phytate, calcium−phytate complex; HAP, histidine acid phosphatase; IPTG, isopropyl β-D-thiogalactopyranoside; ITC, isothermal titration calorimetry; WT, wild type.

10.1021/bi010589u CCC: $20.00
Published on Web 07/19/2001

repulsion causes these acid phytases only to hydrolyze the metal-free form of phytate (*14*, *19*).

Although other biologically diverse phytases also widely distributed in nature and phytate exist as metal−phytate complexes with nutritionally important cations such as Ca^{2+}, Zn^{2+}, and Fe^{2+}, the enzymatic characterizations were mainly focused on HAPs because the most widely used technique to estimate phytase activity is to measure the release of inorganic phosphorus with sodium phytate as substrate. Therefore, the screening of the phytase-producing microorganism and the cloning of the phytase-encoding gene by this principle led us to find usually the histidine acid phytase, which catalyzes the metal-free form of phytate at acidic pH.

Recently, two highly thermostable phytases have been characterized, and the corresponding genes have been cloned from the *Bacillus* species (*20*, *21*). The enzymes have 93% homology on the basis of the amino acid level but do not have sequence homology with other histidine acid phosphatases or other phosphatases, indicating that neither of these contains the active site motif found in HAPs. Unlike other HAPs, they both require Ca^{2+} for activity and show a different pH optimum at 7.0−8.0 (*20*, *22*). Some crude phytase extracts from plants (*23*, *24*) also require Ca^{2+} for activity and have a pH optimum at 7−8.0. This can also occur in the small intestine of humans (*25*), calves (*26*), and rats (*27*). More recently, analysis of the crystal structure of *Bacillus amyloliquefacience* DS11 phytase revealed that the enzyme represents a novel scaffold for the phosphatase activity (*28*).

Although a crystal structure of the phytase from *B. amyloliquefacience* DS11 has been identified and the enzyme requires calcium for activity, a detailed catalytic mechanism of the phytases has not yet been reported. Furthermore, the precise mechanism of how the calcium−phytate complex is hydrolyzed by the phytases has not been introduced in the literature. Therefore, understanding the substrate specificity of the Ca^{2+}-dependent phytases will be invaluable for the understanding of how the calcium−phytate complex is processed in biological systems.

In this study, we have discovered a novel kinetic mechanism of the phytase, which can only hydrolyze the calcium−phytate complex as a true substrate. Moreover, results presented in this paper describe essential activation of phytase and identification of essential amino acid residues for the binding of Ca^{2+} and/or substrate by site-specific mutagenesis.

EXPERIMETAL PROCEDURES

Materials. Plasmid DNA was prepared using Qiagen miniprep kits (Qiagen, Inc., Valencia, CA). Restriction and PCR fragments were purified from agarose gels using the QIAquick gel extraction kit (Qiagen, Inc., Valencia, CA). All other reagents were obtained from Sigma unless otherwise indicated.

Site-Specific Mutagenesis. Site-specific mutagenesis was performed using a Quikchange site-directed mutagenesis kit (Stratagene) and the GeneAmp PE9700 thermal cycler (Perkin-Elmer). Plasmid $pEPK_2$6×His containing the mature gene of phytase was used as the template for mutagenesis (*28*). The following oligonucleotides were used as mutagenic primers: D55A, 5′-GCCGGTGATGCAGCGGCTGATCCTGCGATTTGG-3′; K76E, 5′-TTGATCACAACCAATGAAAATCAGGCTTAGC-3′; K76R, 5′-TTGATCACAACCAATCGAAAATCAGGCTTAG C-3′; R122E, 5′-GCGGCGGCATCCAATGAGTCTGAAGGAAAGAAT-3′; R122K, 5′-CGGCGGCATCCAATAAGTCAGAAGGAAAGAAT-3′; Y159A, 5′-GCAATTGATGAAGTAGCCGGCTTCAGCTTGTAC-3′; Y159F, 5′-ATTGATGAAGTATTCGGTTTCAGCTTG-3′; Y159H, 5′-GCAATTGATGAAGTACACGGTTTCAGCTTG-3′; E211A, 5′-ATGAATTCTCAGACAGCCGGCATGGCAGCAGAC-3′; E227A, 5′-TATATCGCAGAAGCAGATGAGGCAATCTGGAAG-3′; 258A, 5′-GGCAGGCATTTGACCCCTGCTATTGAAGGACTG-3′; E260A, 5′-TTAACCCCTGATATTGCCGGCCTGACGATTTAC-3′; D314A, 5′-GGCACAAGCGATACAGCCGGCATTGACGTTCTG-3′. After PCR, the amplified DNA fragments were ligated by T4 DNA ligase. The ligation mixture was used to transform competent cells of *E. coli* XL1 Blue. The colonies were isolated, and the plasmids were obtained using Qiagen miniprep kits. The DNA sequence of the mutated gene was verified by DNA sequencing.

Overexpression and Purification of N-Terminal His-Tagged Phytase. Plasmids were introduced into competent *E. coli* BL21 (DE3) cells. Cells were initially grown in 50 mL of LB−ampicillin (100 μg/mL) for 8 h at 37 °C. Inocular were added to 2 L of LB−ampicillin (100 μg/mL). The large cultures were immediately moved to an incubator at 30 °C. When the culture reached an A_{600} of 0.6−1.0, isopropyl β-D-thiogalactopyranoside (IPTG) was added at a final concentration of 1 mM to induce 6×His-tagged wild-type phytase as well as phytase mutants. After 3−4 h, cells were harvested and lysed by sonication in equilibrium buffer (50 mM Tris-HCl, pH 7.5, 250 mM NaCl, 10 mM imidazole). Cell debris was removed by two consecutive centrifugations at 4500*g* for 10 min and at 10000*g* for 10 min at 4 °C. The soluble fraction was loaded onto a HR 10/10 column (Phamarcia) packed with 8 mL of nickel−nitrilotriacetic acid (Ni−NTA) superflow resin (Qiagen). The column was washed with 10 column volumes of equilibration buffer (50 mM Tris-HCl, pH 7.5, 250 mM NaCl, 10 mM imidazole). 6×His-tagged protein was eluted with a 0−150 mM imidazole gradient, and elute fractions were pooled and added to solid ammonium sulfate of a final concentration of 1.7 M. The sample was further loaded onto a HiLoad 16/10 phenyl-Sepharose column and eluted with a 1.7−0 M decreasing gradient of ammonium sulfate. Proteins in the peak fractions were pooled and dialyzed in 50 mM Tris-HCl, pH 7.0. The purity of purified phytase was determined by sodium dodecyl sulfate−polyacrylamide gel electrophoresis (SDS−PAGE) with 4% (w/v) stacking and 12% (w/v) resolving gels as described by Laemmli. All of the results presented in this study were obtained by using 6×His-tagged purified phytase.

Phytase Assay. Phytase activity of wild-type and the mutant enzymes was assayed by measuring the rate of increase in inorganic orthophosphate (P_i) using the modified method of Engelen et al. (*29*), which uses molybdovanadate as coloring reagent.

Isothermal Titration Calorimetry (ITC) Measurements. The binding isotherms of Ca^{2+} to the protein solution were determined by measuring the heat changes accompanying titration of the metal ions into solutions of the relevant sample. The measurements were performed with a Microcal titration calorimeter (Microcal, Inc., Northhampton, MA) as described previously by Wiseman et al. (*30*).

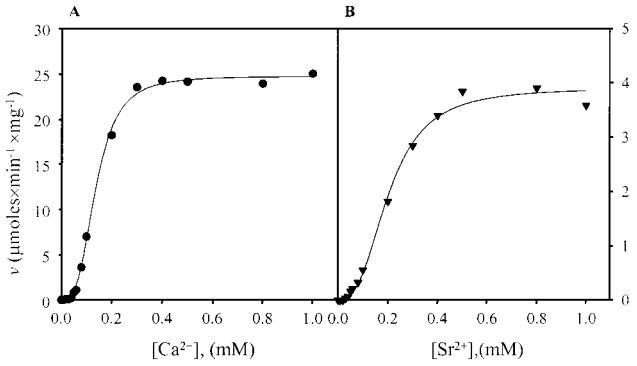

FIGURE 1: Effects of Ca^{2+} (A) and Sr^{2+} (B) on phytase activity. The enzyme was preincubated with increasing concentrations of Ca^{2+} (panel A) or Sr^{2+} (panel B) followed by addition of 1.8 mM phytate preincubated with the same concentration of Ca^{2+} (panel A) or Sr^{2+} (panel B) at 100 mM Tris-HCl (pH 7.0). The curves were generated by fitting to the Hill equation.

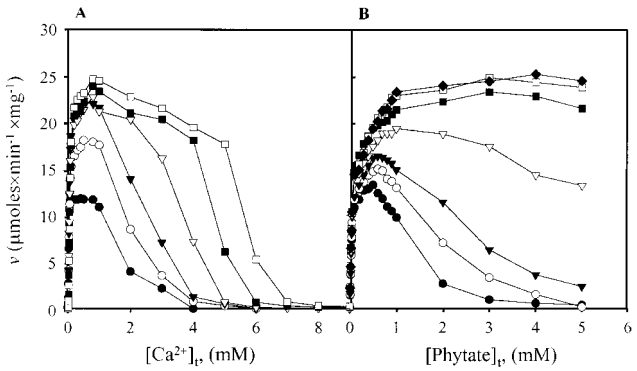

FIGURE 2: Effect of Ca^{2+} concentration (A) or phytate concentration (B) on the rate of phytate hydrolysis (B). For panel A, the Ca^{2+} concentration was varied at the following fixed phytate concentrations: (●) 0.1 mM, (○) 0.2 mM, (▼) 0.4 mM, (▽) 0.6 mM, (■) 0.8 mM, and (□) 1.0 mM. For panel B, the phytate concentration was varied at the following fixed Ca^{2+} concentrations: (●) 0.06 mM, (○) 0.08 mM, (▼) 0.1 mM, (▽) 0.5 mM, (■) 0.8 mM, and (□) 1.0 mM. The rate of phytate hydrolysis under each experimental condition is expressed as v (μmol min^{-1} mg^{-1}).

RESULTS

Effect of Divalent Cations on Phytase Activity. The phytase from *B. amyloliquefaciens* DS11 requires divalent cations such as Ca^{2+} or Sr^{2+} for its catalytic activity. To understand how the cations affect the activity of the phytase, the following studies were carried out. The phytase was preincubated with increasing amounts of Ca^{2+} followed by addition of phytate preincubated with the same concentration of Ca^{2+}. As expected, no detectable phytate hydrolysis was observed when the phytase was added to phytate in the Ca^{2+}-free environment (Figure 1A). Increasing the concentration of Ca^{2+} enhanced the phytase activity at a saturating manner. The results confirmed that Ca^{2+} is required for the phytase to hydrolyze phytate. The Ca^{2+}-dependent increase of reaction rate followed a sigmoidal curve, implying that the activation is mediated by a cooperative interaction of metal ion to the enzyme and/or substrate (Figure 1A). Sr^{2+}, another metal activator of phytase, showed characteristics similar to those of Ca^{2+}, including sigmoidal kinetics at low concentrations (Figure 1B). However, it appears to activate less efficiently than Ca^{2+}. Other divalent cations such as Al^{2+}, Co^{2+}, Cs^{2+}, Cu^{2+}, Mg^{2+}, Mn^{2+}, and Ni^{2+} have no effect on enzyme activation (data not shown).

Effect of Ca^{2+} and Phytate on Phytase Hydrolysis. The results presented in Figure 1 suggest that the phytase requires Ca^{2+} for its activity. The data can be explained in several different ways: Ca^{2+} is required to activate the enzyme; Ca^{2+} binds to phytate and forms an active substrate, calcium−phytate complex; or a combination of both. The following experiments were carried out to sort out the role of Ca^{2+}. Although it would have been ideal if the concentrations of Ca^{2+} and phytate could have been controlled independently to determine their effect on the catalysis, we had to follow a different approach because of the complexity introduced by nonspecific association of Ca^{2+} to both enzyme and substrate. Instead, we have followed London and Steck's approach (*31*) where the rates of reactions were determined by fixing the total concentration of the Ca^{2+} while varying the total phytate concentration, and vice versa.

As discussed earlier, phytase did not show any activity regardless of phytate concentration if there is no Ca^{2+} in the assay medium. When the reaction rates were measured at several different phytate concentrations while varying the Ca^{2+} concentration from 0 to 9 mM, the reaction rate was increased by low concentrations of Ca^{2+} but a significant decrease in the activity was observed as the Ca^{2+} concentration was further increased (Figure 2A). At each fixed phytate concentration, increasing the concentration of Ca^{2+} enhanced the initial velocities of phytase in a saturating manner to yield a Hill coefficient of $h = 3.0 \pm 0.2$. Siegel presented the idea that such a system should follow sigmoidal velocity curves (*32*). The reaction rate was also increased as a function of phytate concentration. However, the reaction rate started to decrease when the concentration of Ca^{2+} was higher than the concentration of phytate (Figure 2A). These results suggest that the enzyme reaction is affected by a complex contribution of unique stoichiometric calcium binding for the activation of enzyme and/or substrate as well as a weak inhibitory effect of free calcium.

Analogously, for Figure 2B, the activity of the phytase was measured at several fixed Ca^{2+} concentrations while phytate was increased from 0 to 5.0 mM. As expected, the rate of reaction increased as the Ca^{2+} concentration increased up to the tested concentration of 1.0 mM. When the fixed Ca^{2+} concentration was lower than 0.2 mM, increasing the concentration of total phytate beyond 1.0 mM resulted in a decreased reaction rate (Figure 2B), indicating that the concentration of free phytate, which is not complexed with Ca^{2+}, increased. The reaction rate started to decrease when the concentration of phytate was greater than 5−10 times the concentration of Ca^{2+} (Figure 2B). The results presented in this and previous sections strongly suggest that the rate of phytate hydrolysis depends on the relative concentrations of both Ca^{2+} and phytate. These results imply that Ca^{2+} is required not only for the activity of the enzyme but also for the substrate.

Essential Activation by Ca^{2+}. Previous results presented in Figure 2 suggest that the calcium−phytate complex (Ca−phytate) is the true substrate for the phytase. To determine whether Ca^{2+} is also required for the activation of the phytase, the following experiments were carried out. The phytase was preincubated with (to form the enzyme−Ca^{2+} complex) and without Ca^{2+} before the enzyme reaction was assayed with varying concentrations of substrate. In this

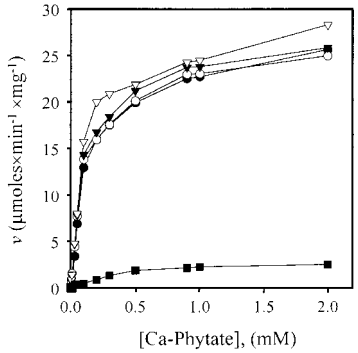

FIGURE 3: Effect of Ca^{2+} on the activity of the phytase. Enzyme was preincubated with the following Ca^{2+} concentrations before determining its activity: (■) no preincubation, (●) 0.01 mM, (○) 0.04 mM, (▼) 0.1 mM, and (▽) 0.4 mM. The rate of phytate hydrolysis was measured using the substrate that was prepared by mixing an equimolar concentration of Ca^{2+} and phytate.

experiment, phytate was premixed with an equimolar concentration of Ca^{2+} and used as a substrate. The result is shown in Figure 3. When the phytase was not pretreated with Ca^{2+}, very little Ca−phytate hydrolysis was observed with slow sigmoidal increase at higher substrate concentration (Figure 3). On the other hand, when the enzyme was preincubated with Ca^{2+}, the reaction rate was greater by an order of magnitude, and the substrate concentration dependency of the reaction became hyperbolic as compared to the sigmoidal curve of the Ca^{2+} free enzyme (Figure 3). The results confirmed that the Ca^{2+} was acting as an essential activator for the phytase; i.e., only enzyme complexed with Ca^{2+} was catalytically active (*32*). The small detectable activity by the Ca^{2+}-free enzyme at higher substrate concentration was probably due to the transfer of small amounts of Ca^{2+} from the substrate to the enzyme.

Inhibition by Free Ca^{2+} and Free Phytate. Ca^{2+} is not only an essential activator for the enzyme but is also required as a part of the substrate. At higher concentrations of either Ca^{2+} or phytate, the rate of reaction was decreased as the concentrations of free Ca^{2+} or free phytate were increased (Figure 2); i.e., excess amounts of free Ca^{2+} or free phytate, not complexed with each other, can inhibit the enzyme reaction. To understand the mode of inhibition in more detail, the effect of additional Ca^{2+} on the rate of Ca−phytate hydrolysis was measured, and the result is shown in Figure 4A. As expected, increasing the Ca^{2+} concentration from 0.4 to 3.0 mM caused a substantial inhibition of phytase activity (Figure 4A). Double reciprocal analysis showed that the apparent K_m increased as the free Ca^{2+} concentration increased while the apparent V_{max} remained constant (Figure 4C). The result confirms that free Ca^{2+} acts as a competitive inhibitor. The K_i value obtained from these results is very high at around 0.97 mM, suggesting that Ca^{2+} extends weak inhibition to the enzyme.

Similarly, the effect of additional phytate on the rate of Ca−phytate hydrolysis was measured by adding free phytate into the reaction mixture. As shown in Figure 4B, the inhibitory effect of free phytate on the rate of Ca−phytate hydrolysis was reproduced. The inhibition by free phytate can result for several reasons: free phytate might act as a weak competitive inhibitor by binding to the catalytic site of the enzyme, or phytate might chelate Ca^{2+}, which acts as an essential activator of the enzyme. The results discussed

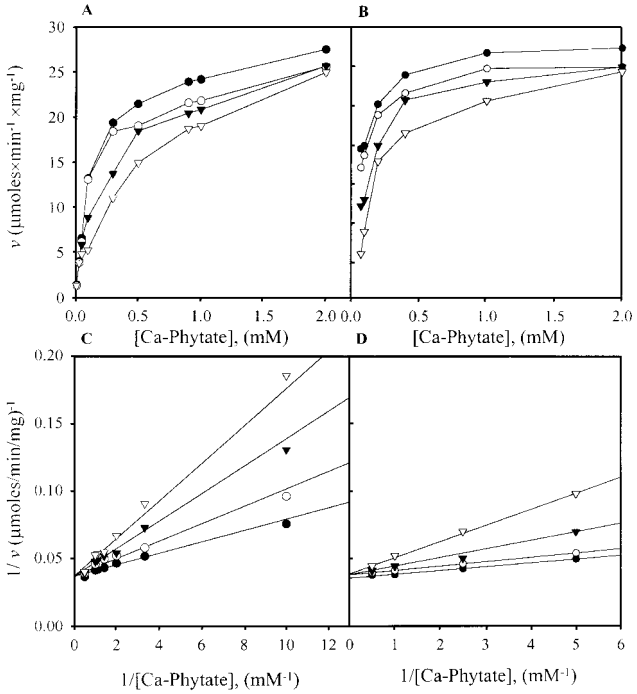

FIGURE 4: Inhibition of phytate hydrolysis by free Ca^{2+} (A) or phytate (B). The rate of phytate hydrolysis was measured in the presence of varying concentrations of Ca^{2+}, (●) 0.4 mM, (○) 1.0 mM, (▼) 2.0 mM, and (▽) 3.0 mM, or in the presence of varying concentrations of phytate, (●) 0 mM, (○) 3.0 mM, (▼) 4.5 mM, and (▽) 6.0 mM. Panel C is a double reciprocal plot of the data from panel A. Panel D is a double reciprocal plot of the data from panel B. The rate of phytate hydrolysis was measured using the substrate that was prepared by mixing an equimolar concentration of Ca^{2+} and phytate.

below suggest that free phytate is a weak competitive inhibitor rather than chelating Ca^{2+}. Double reciprocal analysis shows that the apparent K_m was increased as the free phytate concentration increased whereas the apparent V_{max} remained constant (Figure 4D). The result confirms that free phytate acts as a competitive inhibitor by binding to the active site of the Ca^{2+}-activated phytase. The K_i value (2.30 mM) obtained from these results is higher than the K_i value from Ca^{2+} inhibition kinetics, suggesting that inhibition by free phytate is even weaker than that by free Ca^{2+}.

Identification of Essential Residues for the Binding of Ca^{2+} and Substrate. To confirm the role of essential amino acid residues in the active site, seven amino acid residues critical for Ca^{2+} binding, i.e., Asp55, Tyr159, Glu211, Glu227, Asp258, Glu260, and Asp314, and two additional amino acid residues responsible for substrate binding, i.e., Lys76 and Arg122, were selected for site-specific mutagenesis on the basis of published structural information (*28*). The purified mutant was analyzed with far-UV circular dichroism to make sure that the mutation did not introduce significant change in the folded structure. Table 1 summarizes the kinetic parameters obtained from wild-type (WT) and all mutant phytases. Most of the mutations resulted in decreased activity. Particularly, the mutation of three Ca^{2+}-binding residues at Glu211, Glu260, and Asp314 led to complete loss of activity regardless of the concentration of Ca^{2+}, suggesting that these residues are essential for the catalytic activity. Mutation of the tyrosine 159 residue with phenylalanine resulted in complete loss of activity, while mutation with alanine or histidine resulted in 16 906- and 3537-fold respective

Table 1: Kinetic Parameters for the Wild-Type and Mutant Phytases

enzyme	k_{cat} (min^{-1})	K_m (mM)	k_{cat}/K_m (mM^{-1} min^{-1})	relative activity (%)
wild type	992.48 ± 5.20	0.138 ± 0.022	7191.88	100
D55A	2.08 ± 0.04	0.914 ± 0.019	2.28	0.21
K76E	2.52 ± 0.16	0.967 ± 0.026	2.61	0.26
K76R	2.96 ± 0.04	11.995 ± 1.337	0.25	0.30
R122E	484.40 ± 1.08	2.505 ± 0.041	193.37	48.81
R122K	196.76 ± 1.80	3.046 ± 0.130	64.60	17.11
Y159A	3.68 ± 0.04	8.661 ± 1.089	0.43	0.37
Y159F	*a*	*a*	*a*	*a*
Y159H	1.88 ± 0.04	0.934 ± 0.074	2.01	0.19
E211A	*a*	*a*	*a*	*a*
E227A	92.20 ± 0.16	0.747 ± 0.035	123.43	9.29
D258A	207.16 ± 1.12	3.542 ± 0.103	58.47	20.87
E260A	*a*	*a*	*a*	*a*
D314A	*a*	*a*	*a*	*a*

[a] No reaction (<0.1% of the wild-type rate) was observed.

decreases in the apparent k_{cat}/K_m values compared to WT phytase. The published structural information showed that the hydroxyl group at Tyr159 plays a critical role in Ca^{2+} binding by governing the coordination number and geometry of Ca^{2+} as well as the coordination of the water molecule to the Ca^{2+} (*28*). Mutation of D55A, E227A, and D258A resulted in 3179-, 58-, and 123-fold respective decreases in the apparent k_{cat}/K_m values relative to that of WT enzyme. The apparent k_{cat} values of the D55A, E227A, and D258A mutations decreased 477-, 10.8-, and 4.8-fold, respectively, whereas the apparent K_m values were increased 6.6-, 5.4-, and 25.7-fold compared with WT phytase. These results further support the idea that the calcium-binding amino acid residues are playing a critical role for the activity of the enzyme.

K76 and R122, amino acid residues for substrate binding, were also critical for the activity, as expected. The k_{cat} values of K76R and K76E mutants were decreased by 335- and 393-fold, respectively, whereas K_m values were increased 87- and 7-fold compared to WT phytase (Table 1). The k_{cat} values of R122E and R122K mutants were decreased only 2- and 5.8-fold, respectively, whereas K_m values were increased 18- and 22-fold compared to WT phytase. These results support the involvement of K76 and R122 at the phosphate binding structural motif as recently proposed by structural analysis (*28*).

Isothermal Titration Calorimetric Analysis. Mutation in the Ca^{2+}-binding sites, i.e., Y159F, E211A, E260A, and D314A at the triadic calcium center, resulted in complete loss of enzymatic activity. To investigate whether the mutation alters the substrate binding process or the catalysis, we have directly determined the thermodynamic parameters of Ca^{2+}-binding relationships for WT and mutant phytases. Calorimetric titrations of WT and three mutant enzymes with a $CaCl_2$ solution were performed at 30 °C. The binding isotherm, which corresponds to a plot of integrated heats as a function of the molar ratio of Ca^{2+}/enzyme, is displayed in Figure 5A. The solid line shows the best-fit curve of the data into the two sets of the site model, which describes ligand binding to three nonidentical independent sites. Analysis of these data yields the dissociation constant (K_d), the number of Ca^{2+} bound per protein molecule (n), and the association enthalpy change (ΔH). The thermodynamic

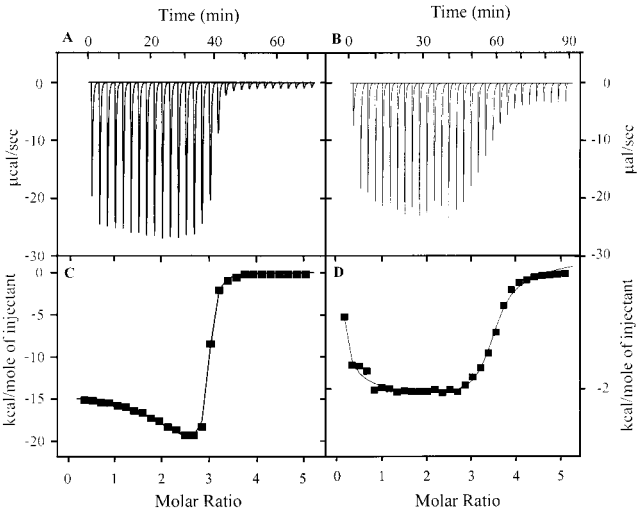

FIGURE 5: ITC analysis of calcium binding to WT phytase (A, B) and phytate (C, D). Panel A shows a calorimetric titration of 4 μL aliquots of 10 mM Ca^{2+} into 0.16 mM WT phytase in 100 mM Tris-HCl buffer (pH 7.0) at 30 °C. Panel B displays the heat exchanged per mole of titrant versus the ratio of the total concentration of the ligand to the total concentration of the protein. The solid line shows the best-fit curve of the data into the two sets of the site model. Panel C shows a calorimetric titration of 2 μL aliquots of 120 mM Ca^{2+} into 1.0 mM phytate solution in 100 mM Tris-HCl buffer (pH 7.0) at 30 °C. Panel D displays the heat exchanged per mole of titrant versus the ratio of the total concentration of the ligand to the total concentration of the phytate solution. The solid line shows the best-fit curve of the data into the sequential binding sites model.

Table 2: Thermodynamic Parameters for the Binding of Ca^{2+} to WT and Mutant Phytase Determined by Isothermal Titration Calorimetry[a]

parameter	site	wild type	E211A	E260A	D314A
K_{d1} (nM)	I	656	1147	1316	803
n_1		0.95	0.88	0.35	0.46
ΔG_1 (kcal/mol)		−8.59	−8.25	−8.16	−8.46
ΔH_1 (kcal/mol)		−23.48	−22.31	−23.38	−21.75
ΔS_1 (cal/mol)		−49.13	−46.41	−50.23	−43.84
K_{d2} (nM)	II, III	97	116	97	132
n_2		1.95	1.59	1.02	0.73
ΔG_2 (kcal/mol)		−9.74	−9.63	−9.72	−9.54
ΔH_2 (kcal/mol)		−14.30	−14.42	−14.27	−13.36
ΔS_2 (cal/mol)		−15.06	−15.82	−14.99	−12.60

[a] The n value represents the number of bound Ca^{2+} ions per protein molecule. The thermodynamic parameters are given for the association reaction.

parameters corresponding to Ca^{2+} binding to WT and mutant phytase are listed in Table 2. Results showed that there are three Ca^{2+}-binding sites in the WT phytase, one with low affinity (K_d = 656 nM) and two others with high affinity (K_d = 97 nM). The E211A, E260A, and D314A mutants displayed large decreases in K_{d1} while these mutants displayed a small decrease in the K_{d2} relative to WT phytase (Table 2). E211A, E260A, and D314A mutants showed both low-affinity site stoichiometry of 0.88, 0.35, and 0.46 mol and high-affinity site stoichiometry of 1.59, 1.02, and 0.73 mol per mole for each mutant, respectively. In summary, the mutants had both a decreased binding affinity and a decreased number of Ca^{2+} binding. The data suggest that the mutation of these residues resulted in a complete loss of enzymatic activity primarily due to the poor binding of the first Ca^{2+} to the low-affinity site.

In a separate experiment, ITC studies were carried out to determine how many Ca^{2+} are required to make an ideal calcium−phytate complex for the substrate and to determine each Ca^{2+}-binding constant. The binding isotherm, showing the integrated heats as a function of the molar ratio of Ca^{2+}/phytate, is displayed in Figure 5B. The solid line represents the best-fit curve of the data into the sequential binding site model, which describes the binding sites that are equivalent and independent since the first ligand to bind has more empty sites of the same kind to choose from than does the second ligand, etc. The analysis of the data yields the dissociation constants and the number of Ca^{2+} bound per phytate molecule. The result obtained from this analysis suggested that 4 mol of Ca^{2+} could bind to 1 mol of phytate. The dissociation constants for 1Ca−phytate, 2Ca−phytate, 3Ca−phytate, and 4Ca−phytate were 2.22, 34.60, 0.69, and 248.0 μM, respectively.

DISCUSSION

Recently, two highly thermostable phytases have been characterized, and the corresponding genes have been cloned from the *Bacillus* species (*20*, *21*). The enzymes have 93% homology on the amino acid level. These enzymes have similar biochemical characteristics when compared with other *Bacillus* phytases (*19*, *20*) and several other phytases from *Typha lattifolia* pollen (*33*), *Lilium longiflorum* pollen (*24*, *34*), and some legume seeds (*23*). However, the biochemical characteristics are different from previously well-characterized histidine acid phytases from *E. coli* (*35*) and fungi (*36*, *37*) because the enzymes require divalent metal ions such as Ca^{2+} or Sr^{2+} for catalytic activity. In fact, a high concentration of Ca^{2+} is known to decrease the activity of the histidine acid phytases (*14*, *38*, *39*). For the same reasons, EDTA readily inactivates *Bacillus* phytases (*20*, *22*, *40*, *41*), whereas EDTA stimulates histidine acid phytases (*14*, *38*). In addition to these differences, these phytases have a pH optimum at 7.0−8.0 while histidine acid phytase showed acidic pH optima. In terms of substrate specificity, the Ca^{2+}-dependent phytases are very specific for phytate, while histidine acid phytases have broad substrate specificity for natural substrate as well as synthetic phosphate esters (*14*, *42*).

Analysis of the crystal structure indicated that a novel scaffolding architecture of a six-bladed propeller for phosphatase activity and that a triadic Ca^{2+} center at the active site cleft provide a favorable electrostatic environment for the metal phytate complex (*28*). This is very different from the active site of histidine acid phytase, which is mostly occupied by positively charged groups for favorable binding and hydrolysis of metal-free phytate (*19*). Although Ca^{2+}-dependent phytases are widespread in nature and phytic acid exists primarily as a calcium−phytate complex, the catalytic properties of Ca^{2+}-dependent phytase have not been well understood.

The results presented in this report demonstrate that phytase requires Ca^{2+} not only as an essential activator but also as part of the calcium phytate complex. X-ray crystallography studies demonstrated the existence of three Ca^{2+}-binding sites at the active site cleft (*28*). Consistently, ITC studies in this report showed that there are three Ca^{2+}-binding sites that are required for the activation of the phytase (Figure 1A, Table 2). This confirms the hypothesis that Ca^{2+} reduces the negative charge around the active site cleft such that phytate neutralized by Ca^{2+} can easily fit to the active site (*28*). In separate experiments, site-specific mutagenesis of amino acid residues at Y159, E211, E260, and D314, which are essential for calcium binding, resulted in complete loss of the enzyme's catalytic activity (Table 1). ITC studies of these mutant enzymes suggest that enzymatic activity loss is primarily due to the poor binding of the first Ca^{2+} to a low-affinity Ca^{2+}-binding site (Table 2). Taken together, Ca^{2+} acts as an essential activator for the calcium phytate hydrolysis by proper binding of substrate to the enzyme's active site. Even though the phytase appears to bind other divalent cations such as Mg^{2+} (0.65 Å) and Co^{2+} (0.74 Å) (*28*), these metal ions could not activate the phytase because they have a smaller ionic radius compared with Ca^{2+} or Sr^{2+}. The unique ability of Ca^{2+} (0.99 Å) or Sr^{2+} (1.12 Å), among other divalent cations, to activate phytase may be due to a similar ionic radius (*43*, *44*). Other properties of Ca^{2+}- and Sr^{2+}-coordinated water could be also significant. This type of essential activation is very similar to the enzymes that require free Mg^{2+} for their biological activity (*32*).

In addition to its role as an essential activator, Ca^{2+} turned out to play another important role as a substrate activator in the formation of the calcium−phytate complex. Results presented in this report show that the phytase does not effectively hydrolyze phytate when there is not a sufficient amount of Ca^{2+} present. Phytate is well-known as a chelator and forms a calcium−phytate complex (*45*). The interaction of Ca^{2+} and phytate is very complex so the determination of the overall binding constants for Ca^{2+} and phytate requires a complicated calculation with proper dissociation constants. Previously, the overall binding constants (K_0) for Ca^{2+} and phytate have been reported to be 2.8×10^3 by using both potentiometric and titration microcalorimeters (*46*). The current thermal data show that Ca^{2+} sequentially binds to phytate; i.e., 4 mol of Ca^{2+} could bind to 1 mol of phytate to yield four different dissociation constants (Figure 5B). The crystallographic study showed that the phytate structure has the phosphates arranged axially in positions 1, 3, 4, 5, and 6 and equatorially in position 2 (*47*). A ^{31}P NMR study by Emsley and Niazi was able to determine the order of proton removal from phytate (*48*). With previous studies and present ITC studies, we can assume that Ca^{2+} is bound with paired oxo dianions of phosphoryl groups and that binding will occur to the axial form. The first binding step would be the phosphoryl group at P5 and P4 or P6, which indicates why Ca^{2+}-dependent phytase initially hydrolyzes at the C_5 atom of the inositol ring of a phytate molecule (*34*). A second Ca^{2+} might bind between P2 and P6, and a third Ca^{2+} might bind between P1 and P3 (Scheme 1).

The results from kinetic studies in this report indicate that the maximal phytase activity was reached when the concentration of the calcium−phytate complex was high while the concentrations of free Ca^{2+} and free phytate were at a minimum (Figure 2A). The pH dependence of phytase activity also indicated that the phytase is most active around pH 6.5−8.0 but required more Ca^{2+} as the pH was decreased (data not shown). This is probably due to the protonation of Ca^{2+}-binding residues in the enzyme and phosphate groups in the substrate, which makes the binding of Ca^{2+} more difficult. This is supported by a lower Ca^{2+} requirement at

Scheme 1: Substrate Binding Scheme to the Active Site of Phytase

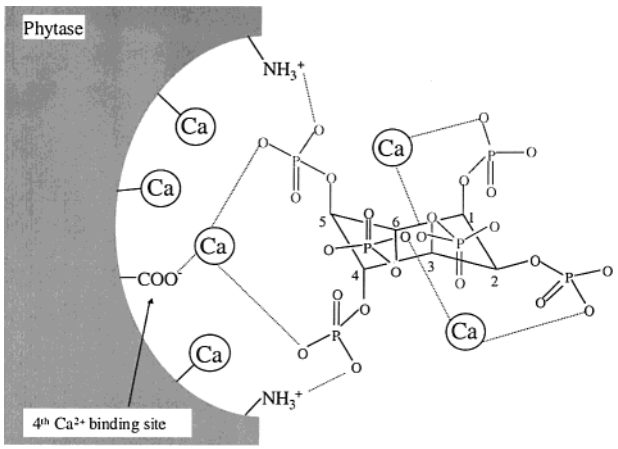

higher pH, where these groups will be ionized for easier formation of Ca^{2+}−enzyme and/or Ca^{2+}−phytate complexes.

Excess amounts of Ca^{2+} turned out to inhibit the phytase activity (Figure 2A). The analysis of the data from Figure 2A suggests that the reaction rate was increased up to the point where all of the Ca^{2+} was converted to a calcium−phytate complex, but above this point the reaction rate was decreased as free Ca^{2+} increased. This indicates that excess amounts of free Ca^{2+} are responsible for the inhibition. Inhibition kinetics showed that the Ca^{2+} increased the apparent K_m but does not affect the apparent V_{max} (Figure 5B), which indicates that Ca^{2+} is a competitive inhibitor of the enzyme; i.e., free Ca^{2+} will preoccupy the active site and inhibit the substrate from binding to the active site.

Excess amounts of free phytate also inhibited the reaction when there was not enough Ca^{2+} present (Figure 2B). This inhibition was diminished when sufficient Ca^{2+} was added. The inhibition kinetics confirmed that the free phytate also acts as a competitive inhibitor (Figure 4B). Considering a favorable electrostatic interaction between the positively charged amino groups of the enzyme's active site and the negatively charged phosphate groups of the calcium−phytate complex, it is likely for the free phytate to bind weakly at the active site of the enzyme.

The pH profiles for the kinetic parameters of phytase suggest that hydrolysis of the calcium−phytate complex is facilitated by acid−base with three ionizing groups that are important for the binding of essential Ca^{2+} and calcium−phytate complex (data not shown). The pK_a values determined from log V and V/K were found to be 3.95 and 9.54, where the pK_a values of 3.95 likely reflect the deprotonation of glutamate or aspartate moieties involved in essential Ca^{2+} binding, and the pK_a value of 9.54 represents the protonated amino group involved in the binding of the phosphate groups of the calcium−phytate complex. Site-specific mutagenesis of the Ca^{2+}-binding amino acid residues and the substrate binding amino acid residues resulted in a significant decrease of the enzyme's activity, which confirmed the critical role of these residues (*28*).

On the basis of the results provided in this report and previous publications, the substrate−enzyme binding scheme shown in Scheme 1 is proposed. Three Ca^{2+} will bind to the Ca^{2+}-binding sites in the active site and create an ideal conformation and charge distribution for the substrate to fit in. The substrate, calcium−phytate complex, will bind to the active site. The fourth Ca^{2+}-binding site will be occupied by a substrate's Ca^{2+}, and the partial negative changes of the phosphate groups will interact with the amino groups of lysine and arginine at the active site.

Scheme 2: Kinetic Scheme for the Hydrolytic Activity from *B. amyloliquefaciens* DS11 Phytase

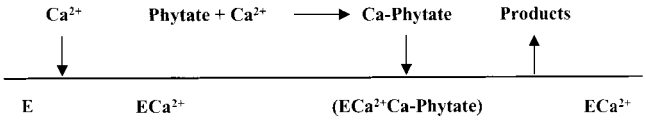

In summary, the following characteristics of *B. amyloliquefaciens* DS11 phytase have been observed in this research: (1) Ca^{2+} serves as an essential activator of the enzyme, i.e., 3 mol of Ca^{2+} are required per mole of the enzyme; (2) the calcium−phytate complex is the true substrate; (3) free Ca^{2+} serves as a competitive inhibitor; (4) free phytate can inhibit the phytase. The proposed kinetic scheme for the rapid equilibrium ordered mechanism for the hydrolytic activity from *B. amyloliquefaciens* DS11 is postulated in Scheme 2.

REFERENCES

1. Reddy, N. R., Sathe, S. K., and Salunkhe, D. K. (1982) *Adv. Food Res. 28*, 1−92.
2. Heaney, R. P., Weaver, C. M., and Fitzsimmons, M. L. (1991) *Am. J. Clin. Nutr. 53*, 745−747.
3. Sandstrom, B., and Sandberg, A. S. (1992) *J. Trace Elem. Electrolytes Health Dis. 6*, 99−103.
4. Lonnerdal, B., Bell, J. G., Hendrickx, A. G., Burns, R. A., and Keen, C. L. (1988) *Am. J. Clin. Nutr. 48*, 1301−1306.
5. Hallberg, L. (1989) *Am. J. Clin. Nutr. 50*, 598−604 (discussion 604−606).
6. Torre, M., Rodriguez, A. R., and Saura-Calixto, F. (1991) *Crit. Rev. Food Sci. Nutr. 30*, 1−22.
7. Navert, B., Sandstrom, B., and Cederblad, A. (1985) *Br. J. Nutr. 53*, 47−53.
8. Brune, M., Rossander-Hulten, L., Hallberg, L., Gleerup, A., and Sandberg, A. S. (1992) *J. Nutr. 122*, 442−449.
9. Spiers, I. D., Freeman, S., Poyner, D. R., and Schwalbe, C. H. (1995) *Tetrahedron Lett. 36*, 2125−2128.
10. Phillippy, B. Q., White, K. D., Johnston, M. R., Tao, S. H., and Fox, M. R. (1987) *Anal. Biochem. 162*, 115−121.
11. Burford, N. T., Nahorski, S. R., Chung, S. K., Chang, Y. T., and Wilcox, R. A. (1997) *Cell Calcium 21*, 301−310.
12. DeLisle, S., Radenberg, T., Wintermantel, M. R., Tietz, C., Parys, J. B., Pittet, D., Welsh, M. J., and Mayr, G. W. (1994) *Am. J. Physiol. 266*, C429−436.
13. Shen, X., Weaver, C. M., Kempa-Steczko, A., Martin, B. R., Phillippy, B. Q., and Heaney, R. P. (1998) *J. Nutr. Biochem. 9*, 298−301.
14. Wyss, M., Brugger, R., Kronenberger, A., Remy, R., Fimbel, R., Oesterhelt, G., Lehmann, M., and van Loon, A. P. (1999) *Appl. Environ. Microbiol. 65*, 367−373.
15. Mullaney, E. J., and Ullah, A. H. (1998) *Biochem. Biophys. Res. Commun. 251*, 252−255.
16. Van Etten, R. L., Davidson, R., Stevis, P. E., MacArthur, H., and Moore, D. L. (1991) *J. Biol. Chem. 266*, 2313−2319.
17. Ostanin, K., Harms, E. H., Stevis, P. E., Kuciel, R., Zhou, M. M., and Van Etten, R. L. (1992) *J. Biol. Chem. 267*, 22830−22836.
18. Ostanin, K., and Van Etten, R. L. (1993) *J. Biol. Chem. 268*, 20778−20784.
19. Lim, D., Golovan, S., Forsberg, C. W., and Jia, Z. (2000) *Nat. Struct. Biol. 7*, 108−113.
20. Kerovuo, J., Lauraeus, M., Nurminen, P., Kalkkinen, N., and Apajalahti, J. (1998) *Appl. Environ. Microbiol. 64*, 2079−2085.

21. Kim, Y. O., Lee, J. K., Kim, H. K., Yu, J. H., and Oh, T. K. (1998) *FEMS Microbiol. Lett. 162*, 185−191.
22. Kim, Y. O., Kim, H. K., Bae, K.-S., Yu, J. H., and Oh, T. K. (1998) *Enzyme Microb. Technol. 22*, 2−7.
23. Scott, J. J. (1991) *Plant Physiol. 95*, 1298−1301.
24. Scott, J. J., and Loewus, F. A. (1986) *Plant Physiol. 82*, 333−335.
25. Sandberg, A. S., and Andersson, H. (1988) *J. Nutr. 118*, 469−473.
26. Hayakwa, T., Okada, F., Tsutsui, M., Sato, N., and Igaue, I. (1991) *Agric. Biol. Chem. 55*, 651−657.
27. Bitar, K., and Reinhold, J. G. (1972) *Biochim. Biophys. Acta 268*, 442−452.
28. Ha, N. C., Oh, B. C., Shin, S., Kim, H. J., Oh, T. K., Kim, Y. O., Choi, K. Y., and Oh, B. H. (2000) *Nat. Struct. Biol. 7*, 147−153.
29. Englen, A. J., Fred., C., Heeft, v. d., Randsdrop, P. H., and Smit, E. L. (1994) *J. AOAC Int. 77*, 760−764.
30. Wiseman, T., Williston, S., Brandts, J. F., and Lin, L. N. (1989) *Anal. Biochem. 179*, 131−137.
31. London, W. P., and Steck, T. L. (1969) *Biochemistry 8*, 1767−1779.
32. Segel, I. H. (1975) *Enzyme Kinetics: Substrate activator complex is the true substrate*, pp 242−272, John Wiley & Sons, New York.
33. Hara, A., Ebina, S., Kondo, A., and Funagua, T. (1985) *Agric. Biol. Chem. 49*, 3539−3544.
34. Barrientos, L., Scott, J. J., and Murthy, P. P. (1994) *Plant Physiol. 106*, 1489−1495.
35. Greiner, R., Konietzny, U., and Jany, K. D. (1993) *Arch. Biochem. Biophys. 303*, 107−113.
36. Ullah, A. H., and Dischinger, H. C., Jr. (1993) *Biochem. Biophys. Res. Commun. 192*, 747−753.
37. Tomschy, A., Tessier, M., Wyss, M., Brugger, R., Broger, C., Schnoebelen, L., van Loon, A. P., and Pasamontes, L. (2000) *Protein Sci. 9*, 1304−1311.
38. Maenz, D. D., Engele-Schaan, C. M., Newkirk, R. W., and Classen, H. L. (1999) *Anim. Feed Sci. Technol. 81*, 177−192.
39. Pallauf, J., and Rimbach, G. (1997) *Arch. Tierernaehr. 50*, 301−319.
40. Powar, V. K., and Jagannathan, V. (1982) *J. Bacteriol. 151*, 1102−1108.
41. Shimizu, M. (1992) *Biosci. Biotechnol. Biochem. 56*, 1266−1269.
42. Liu, B. L., Rafiq, A., Tzeng, Y. M., and Rob, A. (1998) *Enzymol. Microb. Technol. 22*, 415−424.
43. Dobereiner, A., Schmid, A., Ludwig, A., Goebel, W., and Benz, R. (1996) *Eur. J. Biochem. 240*, 454−460.
44. Christianson, D. W., and Cox, J. D. (1999) *Annu. Rev. Biochem. 68*, 33−57.
45. Graf, E. (1983) *J. Am. Oil Chem. Soc. 60*, 1861−1867.
46. Martin, C. J., and Evans, W. J. (1986) *J. Inorg. Biochem. 27*, 17−30.
47. Barrientos, L. G., and Murthy, P. P. (1996) *Carbohydr. Res. 296*, 39−54.
48. Emsley, J., and Niazi, S. (1981) *Phosphorus Sulfur 10*, 1981.

BI010589U